ChemElectroChem

Chemistry Europe
European Chemical Societies Publishing

Accepted Article

Title: Micromolded Carbon Paste Microelectrodes for Electrogenerated Chemiluminescent Detection on Microfluidic Devices

Authors: Erin Gross, Laura R. Porter, Nicholas R. Stukel, Emily R. Lowry, Leah V. Schaffer, Sai Sujana Maddipati, Dylan J. Hoyt, Sarah E. Stombaugh, Sarah R. Peila, and Charles S. Henry

To be cited as: *ChemElectroChem* 10.1002/celc.202000366

Link to VoR: https://doi.org/10.1002/celc.202000366

WILEY-VCH

WILEY-VCH

ARTICLE

Micromolded Carbon Paste Microelectrodes for Electrogenerated Chemiluminescent Detection on Microfluidic Devices

Erin M. Gross *[a], Laura R. Porter[a], Nicholas R. Stukel[a], Emily R. Lowry[a], Leah V. Schaffer[a], Sai Sujana Maddipati[a], Dylan J. Hoyt[a], Sarah E. Stombaugh[a], Sarah R. Peila[a], and Charles S. Henry[b]

[a] Prof. Erin M. Gross, Ms. Laura R. Porter, Dr. Nicholas R. Stukel, Dr. Emily R. Lowry, Ms. Leah V. Schaffer, Ms. Sai Sujana, Maddipati, Mr. Dylan J. Hoyt, Dr. Sarah E. Stombaugh and Dr. Sarah R. Peila
Department of Chemistry
Creighton University
2500 California Plaza, Omaha, NE 68178
E-mail: ErinGross@creighton.edu

[b] Prof. Charles S. Henry
Department of Chemistry
Colorado State University
Fort Collins, CO 80523

Supporting information for this article is given via a link at the end of the document.

Abstract: Micromolded carbon paste electrodes are easily fabricated, disposable, and can be integrated into microfluidic devices to fabricate inexpensive sensors and biosensors. In this work, carbon paste microelectrodes were fabricated in poly(dimethylsiloxane) using micromolding techniques and were coupled to a microfluidic channel to fabricate electrogenerated chemiluminescent (ECL) sensors. ECL was generated using both the tris(2,2'-bipyridyl)ruthenium(II)-tripropylamine system and the hydrogen peroxide and luminol system. For each of these ECL systems, the sensor fabrication method was optimized, along with key experimental parameters (applied voltage, solution flow rate, buffer species and luminol concentration). The limit of detection (S/N = 3) for TPrA was ~2.4 μM with a linear range of 10-100μM. For hydrogen peroxide the LOD was ~11 μM and the electrodes gave a linear response between 30 μM and 200 μM hydrogen peroxide. Electrodes containing glucose oxidase were fabricated using this new method, demonstrating that glucose could be indirectly detected via generation of hydrogen peroxide by the enzymatic reaction at the micromolded biosensor.

Introduction

During the past two decades, the field of microfluidics has grown immensely. One of the ultimate promises of microfluidics research has been a micro-total-analysis system (μ-TAS), where all laboratory functions (such as pumping, reagent mixing, sample handling and detection) occur on a small chip [1]. A significant aspect of μ-TAS development is the development of miniature detectors that can be integrated onto a chip. Electrochemical methods, such as amperometry, have been shown to be effective detectors for microfluidic devices [2-3]. Electrochemistry is amenable to miniaturization with minimal loss of sensitivity relative to optical methods. Electrodes are also relatively inexpensive to fabricate, making them useful for disposable analytical devices [4-5]. Additionally, some types of electrochemical detectors can be mass-produced easily, making commercialization a reality. Chemiluminescent (CL) detection methods also offer a simple solution to fabrication of low cost sensitive detectors [6]. The technique of electrogenerated chemiluminescence (ECL) [7-8] generates reactive chemiluminescent reagents at an electrode. ECL detection methods possess the simplicity, low cost and ease of miniaturization associated with electrochemical methods plus the additional benefits of the increased sensitivity of luminescent methods [9-11]. For example, DNA and micro-RNA have both been detected at fmol/L levels using metallonanoparticle-enhanced ECL [12-13]. Because the chemiluminescent reagents are generated *in situ* at the working electrode, there is no waiting time for reagents to mix and precise chemical and spatial control is exerted over the reaction. A greater selectivity relative to chemiluminescence can be achieved using the potential applied to the chemical system. In many cases, the CL reagent is also regenerated, reducing analysis cost and simplifying operation.

Carbon electrodes posess advantages of low cost, a wide potential window, and relatively intert electrochemistry [14]. Recently, new approaches for incorporating carbon-based electrodes into microfluidic devices have been reported [4, 15-16]. In one approach [4], carbon paste microelectrodes (CPEs) were fabricated via a method analogous to screen printing in a poly(dimethylsiloxane) (PDMS)-based microfluidic chip. This method employed a mixture of graphite, mineral oil and a PDMS cross-linker as the working, counter and reference electrodes, with the PDMS added to provide physical stability. The low-cost PDMS/carbon-based electrodes were shown to be effective for electrochemical detection applications and could easily be patterned for integration into microfluidic devices. They are also porous and increase the surface area of the electrodes, thus can boost ECL signals. Carbon paste microelectrodes are also amenable to modification, particularly with nanomaterials or other substances that can enhance the ECL signal [17]. In the work presented here, a similar microfluidic chip has been employed for ECL detection. The PDMS-based chip containing the channel and electrode is transparent and planar, making is amenable to alignment with a photomultiplier tube for a simple ECL detection method. Here, samples are injected onto a microfluidic channel which is integrated with an electrochemical cell containing working, counter and reference elctrodes. ECL is generated at the

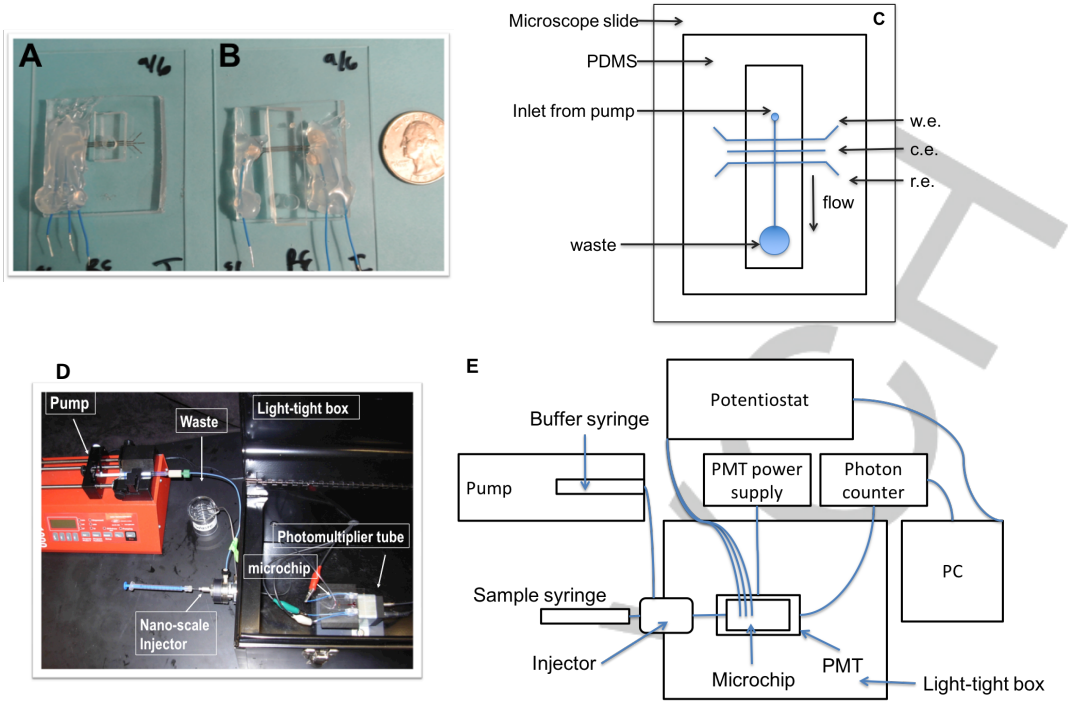

Figure 1. Photographs of carbon paste microelectrodes coupled with a reservoir (A) and a microfluidic flow channel (B); diagram (C) of the microfluidic chip in (B); Photograph (D) and schematic (E) of the microfluidic flow-injection analysis photon counting system.

working electrode and detected through the transparent PDMS-based device. Devices such as these possess the benefits of microfluidics, including low cost, speed, and the potential for portability and automation. In ECL, photons are generated after a heterogeneous electron transfer followed by a homogeneous electron transfer reaction [7-8]. ECL is a useful analytical technique as the photons produced are proportional to the ECL luminophore's concentration and, in the case of co-reactant ECL, are proportional also to the co-reactant concentration. There is also little to no background luminescence, allowing for low detection limits. To generate ECL, the analyte can either be labeled with the chemiluminescent reagent or serve as the co-reactant. ECL has been used as a detection method in both flow-based microfluidic systems and microchip capillary electrophoresis systems [9-10], but has not been as widely applied as other electrochemical methods [2]. Further investigation and development of ECL-based microfluidic and nanofluidic techniques is needed to evaluate its use in micro- and nano scale devices [10,18-19].

In this work we demonstrate the applicability of micromolded carbon paste electrodes for use in $Ru(bpy)_3^{2+}$ and luminol-based electrochemiluminescence detection methods on microfluidic devices. PDMS-based microfluidic devices are an excellent match for ECL detection, as PDMS is transparent in the visible region. With this novel ECL detection system, we can inject nanoliter sized samples onto the microchip, perform stopped flow experiments, or use a reservoir mode for other studies. It is a flexible system amenable to multiple types of experiments, both ECL and electrochemical. The goal of the present work was to optimize the electrochemical and microfluidic system variables for ECL reactions using well-known ECL reactions as models. The first reaction investigated was that of $Ru(bpy)_3^{2+}$ and tripropylamine as oxidative-reduction co-reactant. This type of reaction can be used to detect amines and molecules containing amine functional groups. The detection of biogenic amines can provide information about microbial contamination in foods [20], while many drug molecules contain amine functional groups and can pariticipate in ECL reactions [21-22]. The second reaction investigated was the luminol-hydrogen peroxide ECL reaction, which has many applications to ECL-based biosensors [23]. As a proof of concept, glucose oxidase was incorporated into a CPE and glucose was detected at levels typical in biological samples, such as blood.

Results and Discussion

These carbon paste microelectrodes and microfluidic devices have been used primarily for electrochemical sensing [4] so we wished to investigate their use as ECL sensors. The electrode design and experimental set-up is shown in Figure 1 and described in the Experimental section. We optimized and evaluated the ECL response of the electrodes using the well-characterized $Ru(bpy)_3^{2+}$/tripropylamine and luminol/hydrogen peroxide ECL reactions (Figure S1) [23]. For these ECL reactions, flow system and chemical parameters were systematically varied in order to determine the optimal conditions for generating ECL

Electrode Characterization and Optimization. The fabricated carbon paste microelectrodes were characterized by cyclic voltammetry (CV) to assess both their electrochemical quality in general and their use in $Ru(bpy)_3^{2+}$-amine based ECL reactions. Cyclic voltammograms of the oxidation of $Ru(bpy)_3^{2+}$ at a CPE as a function of scan rate are shown in Figure S2A. The peaks were diffusive in nature and when the peak current is plotted versus square root of scan rate, a linear relationship is shown (Figure S2B), as predicted by the Randles-Sevik Equation for a diffusive system with a reversible reaction [24]. The oxidation is reversible, with an $E_{1/2}$ for the $Ru(bpy)_3^{2+}$ system is around 0.92 V vs Ag/AgCl.

Therefore, $Ru(bpy)_3^{2+}$ reversibly undergoes a diffusion-controlled oxidation to $Ru(bpy)_3^{3+}$ at the CPE's. The other electrochemical data collected for these electrodes, ΔE_p and i_{pa}/i_{pc}, demonstrate reversible behavior but an increased resistance versus a conventional electrode.

$Ru(bpy)_3^{2+}$-Tripropylamine System

Cyclic Voltammetry. The $Ru(bpy)_3^{2+}$/TPrA ECL system has been demonstrated to produce the highest signal in the pH range of 7-8 [25] so all experiments were conducted at pH 7.4. Prior work in our lab established a maximum ECL response with high concentrations of $Ru(bpy)_3^{2+}$ when amine concentration was low [21], so all experiments used 4 mM $Ru(bpy)_3^{2+}$. Under these conditions, ECL could be generated during a CV scan (Figure 2A) of a $Ru(bpy)_3^{2+}$/TPrA solution in a reservoir placed over the electrode. We observe an onset of ECL coinciding with $Ru(bpy)_3^{2+}$ oxidation (Figure S1A, reaction 1) at a potential of ~0.9 V, and see an increase in signal throughout the scan. During the reverse scan, the ECL signal remains fairly constant, indicating the stability of $Ru(bpy)_3^{3+}$ [26], until ~0.9 V where the signal decreases during the course of the scan.

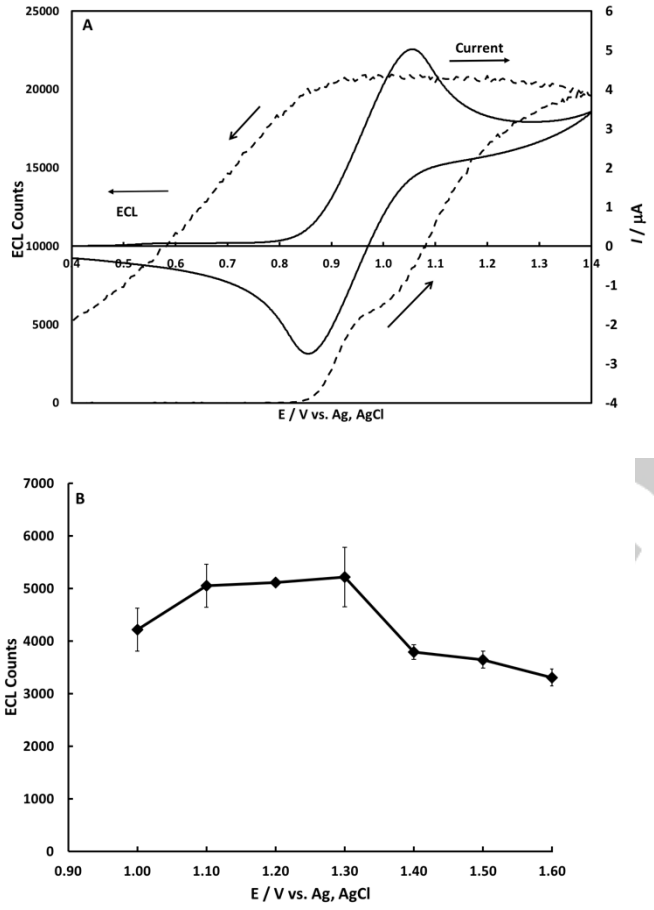

Figure 2. Cyclic voltammogram (solid line) and concurrent ECL trace (dashed line) at a CPE scanned at 0.050 V/s in a reservoir (A) and ECL signal versus potential for injections (n = 3) in the FIA system (B) for a solution containing 4.0 mM $Ru(bpy)_3^{2+}$ and 100 μM TPrA in a 0.15 M PBS (pH 7.4) at a flow rate of 10 μL/min.

Similar CV and ECL responses were observed by Chen and Zu at a glassy carbon electrodes [26]. The mechanism here is likely the co-reactant mechanism reported by many groups [23,26-27] and is shown in Figure S1A. $Ru(bpy)_3^{2+}$ is initially oxidized at the electrode as described above. TPrA can be oxidized homogeneously by the electrogenerated $Ru(bpy)_3^{3+}$ (Figure S1A reaction 2a), leading to a catalytic, EC', route or directly oxidized at the electrode (Figure S1A reaction 2a). Chen and Zu reported that the catalytic oxidation of TPrA by $Ru(bpy)_3^{3+}$ could occur within a relatively thick layer around the electrode. Under our reaction conditions, similar to those of Chen and Zu, the EC' route likely dominates. The oxidized TPrA subsequently forms a free radical (Figure S1A reaction 3). This reducing agent reduces $Ru(bpy)_3^{3+}$ producing an orange ECL from electronically excited $Ru(bpy)_3^{2+}$ at ~620 nm (Figure S1A reactions 4-5). The CV-ECL experiment performed in Figure 2A was repeated at three additional scan rates (0.10, 0.25 and 0.50 V/s), which is shown in Figure S3. At each scan rate, we observed similar temporal behavior of the ECL signal with potential, but did observe a decrease in ECL signal with an increase in scan rate. This observation of an increased ECL signal at longer experiment times is discussed later in this paper in the context of the flow rate dependence. It is important to note that the ECL signal is collected beneath the electrode, indicating that these porous microelectrodes are somewhat transparent, as they allow light to pass through them. When we conducted an experiment where light was collected above the electrode, we observed a factor of two increase in signal. However, this geometry was not as easy to implement as the other. In the future, the microchip and ECL collection system could be redesigned in order to lower detection limits, however the system as shown in Figure 1 was simple and easy to use, with sufficiently high ECL signals. Using this information, 500 nL injections of $Ru(bpy)_3^{2+}$/TPrA solution were injected onto the microchip and oxidized at potentials ranging from 1.0 – 1.6 V. We observed maximum ECL signals over a range of 1.1-1.3 V and used potentials within this range for generating ECL on the flow system moving forward.

We also evaluated the stability of the fabricated reference electrode by modeling the solution conditions during an ECL experiment. Figure S4 shows ten cyclic voltammograms collected for a solution of 100 μM tripropylamine in 4.0 mM $Ru(bpy)_3^{2+}$ in pH 7.4 PBS. We observed good trial-to-trial overlap among the CV peaks, with no more than a 10 mV drift during the course of the experiment.

Flow Rate, Precision and Linearity. The ECL signal of sample injections onto the microchip was found to be flow rate dependent. Over a range of flow rates between 0.5 and 20 μL/min, the ECL intensity was the highest at the slower flow rates, specifically in the range of 2-4 μL/min (Figure 3A). We speculate that the slower flow rates allow more time for the diffusion layer to grow, promoting the EC' mechanism and increasing the ECL signal. This observation is also supported by the CV-ECL scan rate study shown in Figure S3. Again, higher ECL signals were observed at longer experiment times. We observed the highest ECL signal at the slowest scan rate. A thicker diffusion layer would also be expected at slower scan rates, giving the reaction more time to occur, just as with the slower flow rates. At a flow rate of 2 μL/min, each trial initially took around 5 minutes (Figure 3B). Faster analysis times can be achieved by increasing the flow rate slightly

and by further decreasing of tubing and channel lengths leading up to the electrodes. Figure 3B shows the temporal profile of a typical injection, Typically, these electrodes gave precision values of ~3-7% RSD over various concentrations of TPrA in the presence of 4.0 mM $Ru(bpy)_3^{2+}$.

The CPEs responded linearly to TPrA concentration (R^2 = 0.98) over a range of 10-100 μM (Figure 3A inset). The LOD was determined to be ~2.4 μM. The limit of detection is ultimately limited from a background signal that arises from $Ru(bpy)_3^{2+}$ in the buffer. We have observed this background to be small and stable and it could be subtracted from the signal for future analytical work. This detection limit for TPrA is on par with other literature reports on microscale ECL methods and methods using microelectrodes [28-32]. Reported methods are summarized in the supplemental material Table S2.

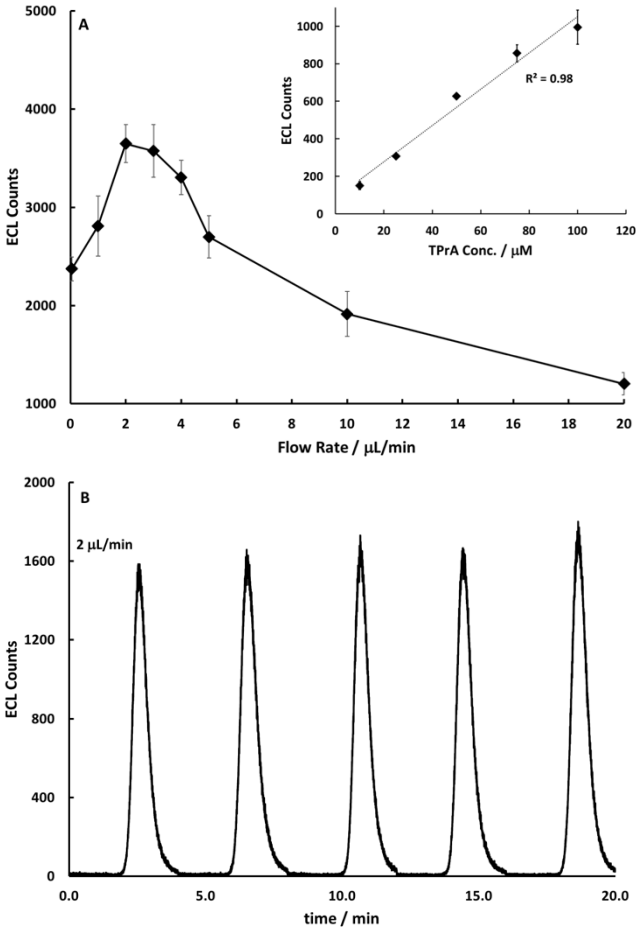

Figure 3. ECL intensity vs. flow rate (A) and individual injections (B) on the carbon paste microelectrode microchip. All solutions injected were 100 μM TPrA and 4.0 mM $Ru(bpy)_3^{2+}$ in 0.15 M PBS pH 7.4. ECL was collected in 100 ms intervals with $E_{applied}$ = 1.2 V. Inset: ECL signal as a function of TPrA concentration at a flow rate of 2 μL/min.

Luminol System

Luminol-based ECL [31] is an attractive method because it detects hydrogen peroxide, a by-product of many enzymatic reactions [32]. The mechanism for luminol ECL has been studied by various groups and depends on the oxidant and/or potential applied [21,33-35]. In general, the steps shown in the supplementary material (Figure S1C) lead to luminol ECL [21]. The reaction occurs most efficiently under alkaline conditions, when luminol has been deprotonated (pK_{a1} = 6.2). The first step in this mechanism is electro-oxidation of the monobasic anion of luminol (LH^-) to the diazoquinone. This species reacts with the oxidant (e.g. peroxide) to produce an intermediate which rapidly decomposes to 3-aminophthalate, the light-emitting species. ECL emission spectra generally show a maximum at 425 nm.

Although luminol alone can generate light under ECL conditions, the additional presence of an oxidant such as hydrogen peroxide increases the amount of light produced, which is desirable for microscale detection. Most applications of luminol ECL focus on detection of the oxidant species, rather than using luminol as an ECL label. Hydrogen peroxide is a frequent target due to its biological importance and association with numerous oxidase enzymes. Many applications involve indirect quantitation of a substrate whose reaction enzymatically produces hydrogen peroxide. A common example is glucose detection. Here, glucose oxidase (GOx) catalyzes the oxidation of glucose, producing hydrogen peroxide (Equation 1). The hydrogen peroxide is subsequently detected by luminol ECL when both species are oxidized at an electrode (Equation 2). The full luminol peroxide ECL mechanism is described in Figure S1.

$$\text{D-glucose} + O_2 \xrightarrow{GOx} \text{gluconate} + H_2O_2 \quad (1)$$

$$H_2O_2 + \text{luminol} \xrightarrow{\text{Electro-oxidation}} \text{3-aminophthalate} + N_2 + \text{light} \quad (2)$$

Glucose oxidase can be readily immobilized onto an electrode. At a properly biased electrode potential and in the presence of the substrate and luminol, ECL is observed and the amount of ECL signal can be related to substrate concentration [34]. Other substrates that produce H_2O_2 in a similar mechanism include substances such as choline, lactate and cholesterol [36-37].

As with the $Ru(bpy)_3^{2+}$-TPrA system, the flow system and chemical parameters were systematically varied in order to determine the optimal conditions for generating ECL. The flow system parameters investigated included the applied potential and flow rate. The chemical parameters studied were the luminol concentration and working and counter electrode binder composition. The buffer type and solution pH used were based on previously reported results [11, 35-36]. The reaction is most efficient at basic pH, but when considering future fabrication of biosensors, the reaction should be at a pH where the enzyme is still active [23,38-39]. A background ECL signal was observed from buffer solutions containing only luminol (no hydrogen peroxide), so additional parameters were evaluated to determine if this background could be minimized.

Cyclic Voltammetry. Cyclic voltammograms were obtained *in reservoir* for the reagents to determine the potentials at which luminol and peroxide oxidize (Figure 4A) at the CPE's. Due to solubility limitations in the veronal buffer the higher concentration solutions required for CV analysis, solutions for CV were prepared in 0.1 M NaOH solution. Broad oxidation waves for both hydrogen peroxide and luminol were observed. Luminol oxidation onset at

~0.5 V and exhibited a wave at ~0.7 V vs. Ag/AgCl while hydrogen peroxide oxidized between 0.8 V and 1.0 V. This voltammetric data is comparable to previous data using the same chemistry but different electrochemical cells [23, 36]. The mixture of the two solutions also exhibited a broad wave corresponding to the oxidations of both species. A CV-ECL trace collected on these solutions *in reservoir* showed a maximum ECL intensity at around 0.5 V (Figure 4A inset).

We also investigated the potential dependence of the luminol system for 500 nL injections in the microfluidic system at lower solution concentrations typical of those used for ECL experiments (Figure 4B). Here we observed the ECL intensity to increase with potential until around 0.9 V, with a maximum intensity in the 0.9 – 1.1 V range. Subsequently, for all injections onto the microfluidic chip, a potential of +1.0 V was applied. When ECL was generated in this manner, the data was peak-shaped, as shown in Figure 5B inset. For all subsequent studies, the data was collected in this manner and the peak light counts determined.

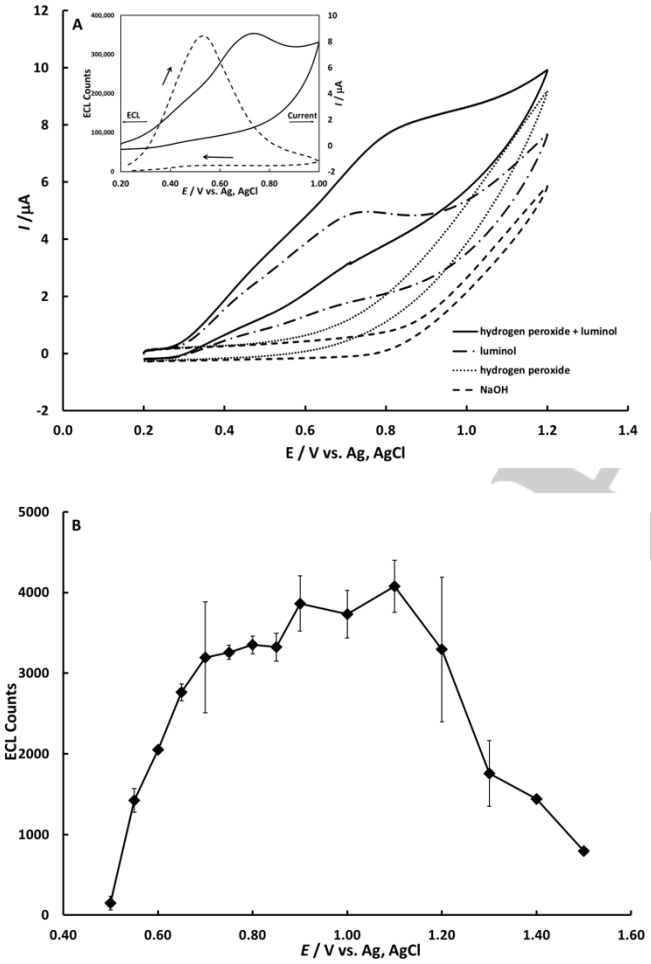

Figure 4. *In reservoir* cyclic voltammograms (A) of 0.1 M NaOH and solutions containing 0.1 M NaOH and the following solutes: hydrogen peroxide, luminol and a hydrogen peroxide/luminol mixture. Inset: CV-ECL scans collected on a 0.1 M NaOH solution containing 2.5 mM hydrogen peroxide and 2.5 mM luminol. All solutes were at a concentration of 2.5 mM and CVs were collected at a scan rate of 0.1 V/s. *In channel* ECL signal versus potential (B) for injections containing 2.5 mM H_2O_2 and 50μM luminol in pH 8.5 veronal buffer at a flow rate of 10 μL/min (n = 3).

Flow Rate Optimization. The system flow rate was varied to determine the rate giving the optimal signal along with a fast analysis time. Initially, flow rates between 5 – 20 μL/min were screened. Upon observing a maximum between 10-15 μL/min, a narrower range was investigated (Figure 5A). The optimal flow rate was determined to be in the range of 10-12 μL/min. In addition to giving a maximum signal, this flow rate allowed sufficient time for the two species to react at the electrode surface while maintaining a relatively fast analysis time. Each sample analysis lasted around one minute as shown in the inset in Figure 5B.

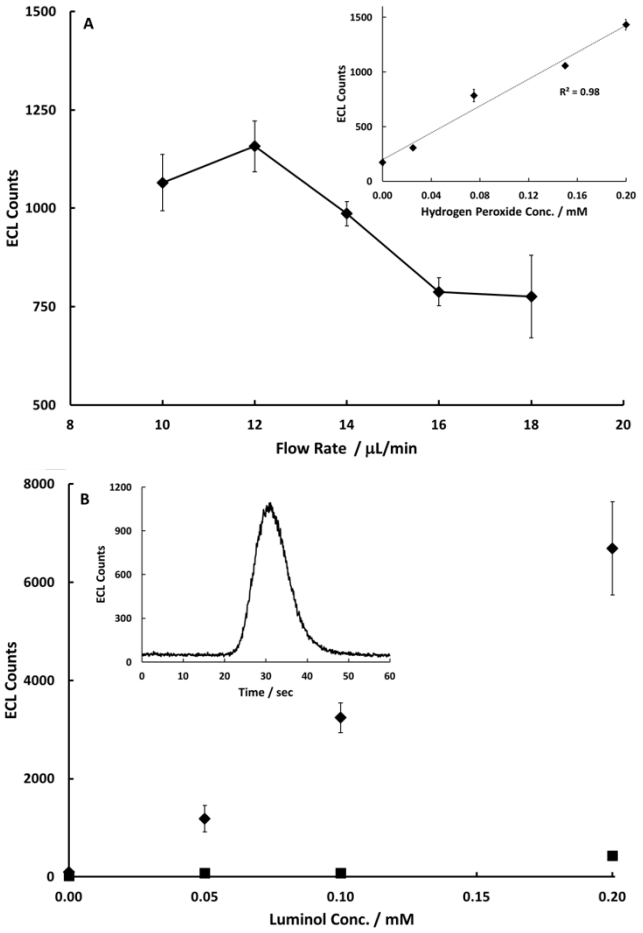

Figure 5. ECL signal as a function of flow rate for 500 nL injections (n = 3) of a solution containing 50 μM luminol and 1.0 mM hydrogen peroxide (A) at an applied potential of 1.0 V. Inset: ECL signal as a function of hydrogen peroxide concentration for 500 nL injections (n = 3) of solutions containing 200 μM luminol in pH 8.5 veronal buffer at a flow rate of 10 μL/min and an applied potential of 1.0 V. ECL signal as a function of luminol concentration for 500 nL injections (n = 3) of solutions containing only luminol (diamonds) and luminol plus 50 μM hydrogen peroxide (squares) in pH 8.5 veronal buffer at 10 μL/min (B). Inset: ECL signal as a function of time for a solution containing 50 μM luminol and 1.0 mM hydrogen peroxide in pH 8.5 veronal buffer at a flow rate of 12.0 μL/min and an applied potential of 1.0 V.

Luminol Concentration. For detection of peroxide, the luminol concentration should be constant during the analysis. However, when generating electrochemiluminescence, a background signal is observed in the absence of peroxide [33], meaning the luminol concentration should be kept low to minimize background signal.

Figure 5B shows the ECL signal generated by both luminol only and luminol plus peroxide solutions as a function of luminol concentration. As expected, the signal for both sets of solutions increases with increasing luminol concentration. However, the CPE's exhibit greater sensitivity to the luminol plus hydrogen peroxide solution. Based on the signal-to-noise ratios, a luminol concentration of 200 μM was used in future experiments.

Hydrogen Peroxide Detection. The precision, linearity, and limit of detection for peroxide detection were determined under the optimized analysis conditions. Figure 5A (inset) shows that the system had a linear response over a range of 50 μM to 200 μM peroxide and a limit of detection (LOD, S/N = 3) of ~11 μM was determined. The detection limit for peroxide in this microfluidic system are similar to luminol-based microscale ECL methods and methods using microelectrodes [29,31-32,38,40]. Reported methods are summarized in the supplemental material Table S2 Typical precision values for 10 sequential injections were ~13% coefficient of variation. These precision values are on par with those reported for similar electrochemical microelectrode-based microfluidic devices [5].

Glucose Biosensor Fabrication and Characterization. Hydrogen peroxide is a product of numerous enzymatic reactions. Enzyme electrodes are commonly used and have been commercialized to electrochemically detect hydrogen peroxide and indirectly measure metabolites such as glucose and lactate [36-37]. The same enzymatic reactions can be used to generate hydrogen peroxide in the presence of luminol and generate ECL [23]. ECL methods have been developed to detect analytes such as glucose, cholesterol and choline [38,39-41]. Various reports exist in the literature for immobilizing enzymes such as glucose oxidase (GOx) or cholesterol oxidase onto an electrode [43-45]. For example, one method involved immobilizing the enzyme in a photo-cross-linkable poly(vinylalcohol)polymer after adsorption on DEAE sepharose anion-exchanger beads [23,38].

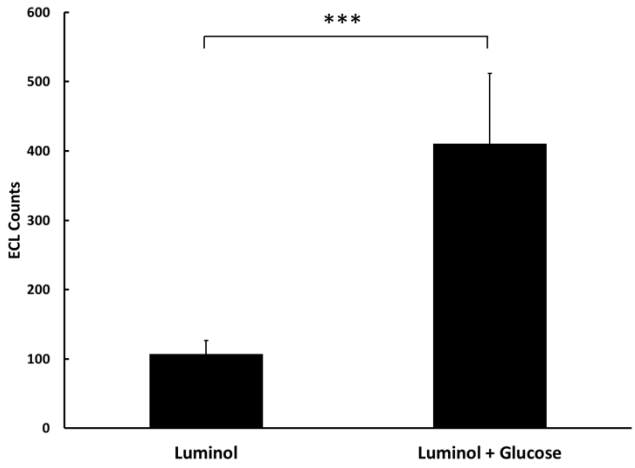

Figure 6. ECL signal for a biosensor containing 10% w/w glucose oxidase from a pH 8.5 veronal buffer containing 10 μM luminol and 10 μM luminol plus 0.1 mM glucose. Flow rate was 5 μL/min with an applied potential of +1.3 V (determined from visually observing ECL signal during a CV). Statistical analysis $p < 0.0001$

In this current work, as a first step, a simple method using the microfluidic CPE chips was investigated. The GOx was mixed into the carbon paste mixture at a concentration of 10% w/w and incorporated into the electrode channel as described in the experimental section. These electrodes were investigated as potential glucose biosensors. When a potential was applied to an electrode in the presence of a solution of only luminol and buffer, a small signal is observed as shown in Figure 6. When 0.1 mM glucose was added to the solution, the resulting signal is enhanced as shown in Figure 6. An unpaired t-test demonstrated the statistical difference in the change in signal. Additionally, these electrodes were found to be stable and produce a signal for at least 40 days. Relative standard deviation values (n = 4) ranged from 4 – 11% for all data sets.

Conclusion

Carbon paste microelectrodes can be used for generation of both $Ru(bpy)_3^{2+}$ and luminol electrogenerated chemiluminescence when incorporated into a microfluidic device. The electrodes were sufficiently robust for incorporation into these devices and could quickly, simply and inexpensively be fabricated. The devices were able to detect tripropylamine, hydrogen peroxide and glucose at reasonable levels in a microfluidic device. The methods were linear, and the devices exhibited an acceptable precision and sensitivity. The CPEs can be easily patterned and modified, showing the potential of these devices as ECL-based chemo- and biosensors. Detection devices such as these could be multiplexed, integrated with other laboratory functions on a chip, or integrated onto an automated device.

Experimental Section

Materials and Reagents. Tris(2,2'-bipyridyl)dichlororuthenium(II) hexahydrate powder was obtained from Strem Chemicals. Tripropylamine (99+%), luminol (3-aminophthalhydrazide, >98.0%), glucose oxidase (Glucose Oxidase from *Aspergillus niger* , Type X-S, lyophilized powder, 100,000-250,000 units/g), graphite powder (<20 μm, synthetic), mineral oil (White, Heavy), and AgCl (99.999%) were obtained from Sigma-Aldrich (St. Louis, MO USA). Monosodium phosphate monohydrate, boric acid, and hydrogen peroxide (30%, ACS Grade) was obtained from Fisher Scientific (Waltham, MA USA). Poly(dimethylsiloxane) (PDMS, Sylgard 184 Silicone Elastomer and Sylgard 184 Silicone Elastomer Curing Agent) was obtained from Dow Corning (Midland, MI, USA). Silver Paint (High Purity) was obtained from Structure Probe, Inc. (West Chester, PA). Veronal buffer (5X Concentrate) was obtained from Lonza (Walkersville, MD USA). All chemicals were reagent grade or higher.

Solutions were prepared fresh for each study. A 0.15 M phosphate buffer solution (PBS, pH 7.4) was the flowing buffer for the initial $Ru(bpy)_3^{2+}$ and TPrA experiments. A 4.0 mM $Ru(bpy)_3^{2+}$ and varying concentrations of TPrA were made in PBS buffer and injected as sample plugs. A veronal buffer at pH 8.5 was used for luminol ECL experiments. The stock veronal buffer (5X) was adjusted to pH 8.5 using 2 M NaOH and diluted to create a working buffer solution. More concentrated luminol solutions for CV analysis were prepared in 0.1 M NaOH. Otherwise, all other solutions of luminol, hydrogen peroxide and glucose were prepared in the diluted veronal buffer (pH = 8.5).

Microchip Fabrication. The PDMS molds for the both the flow channel and CPEs and the were created using rapid prototyping methods [4,46]. The silicon wafers were prepared using previously reported photolithography methods using SU-8 photoresist to create positive relief structures. A straight, 150 μm wide and 50 μm height channel on a silicon

wafer was used to make the flow channel. The silicon wafers for electrode fabrication had working, counter, and reference electrode channels, each 250 µm wide, 50 µm deep, and separated by 600 µm. The PDMS microchip was composed of an electrode base with a flow channel on top, both of which were fabricated by pouring the PDMS mixture onto a silicon wafer containing the electrode or flow channel pattern. Figure 1b-c shows a photograph and a basic diagram of a device. The PDMS was made by mixing a 10:1 ratio by mass of Sylgard 184 elastomer to curing agent. After mixing, the PDMS was poured onto the silicon wafer. After curing the PDMS on the wafer in the oven for two hours at 80°C, the molded PDMS was cut out and removed from the wafer using a razor blade. Holes were punched into each end of the flow channel as follows. A 5 mm biopsy punch was used on one end to create a large hole, which acted as a reservoir for the solution flowing through the channel. A 20-guage blunt tip needle was used on the other end to create a hole for the tubing coming from the nano-injector.

Electrode Fabrication. The cured PDMS electrode base was placed on a double microscope slide for stabilization. The working and counter electrode channels were filled with a carbon paste mixture to create the electrodes. This carbon paste mixture consisted of a 1:1 ratio (by mass) of graphite powder to binder. The binder contained a 1:1 ratio (by mass) of mineral oil and PDMS mixture. Therefore, the final ratio (by mass) was 2:1:1 graphite powder:mineral oil: PDMS mixture. The reference electrode channel was covered using scotch tape, and the carbon paste was then spread into the working and counter electrode channels with a plastic kitchen scraper. The excess paste was removed with scotch tape until there was only paste inside the channels and none on the top of the electrode. At this point, the tape covering the reference electrode channel was removed and the other channels covered. The following paste mixture was added to the reference channel in the same manner: 40% (w/w) graphite powder, 50% binder, 5% (v/w) Ag ink, and 5% AgCl. The electrodes were cured in the oven for 1 hour at 80°C. When glucose oxidase was incorporated into the electrodes (10% w/w), the electrodes were cured overnight at room temperature. Next, copper wires (OK Industries 26 AWG R26B-0100) were stripped at the ends and attached to each electrode using silver paint. After the paint dried, the electrical connection was covered in hot glue using a mini glue gun.

Two different types of fluidic devices were fabricated. The first type was the microfluidic device as just described and shown in Figure 1B-C. A PDMS flow channel was reversibly sealed over the top of the electrode in a perpendicular fashion. The area of electrode exposed to solution here was ~0.0375 mm^2. This chip was integrated into the flow system described in the next section. The second device operated in a reservoir mode, as shown in Figure 1A. This design was used primarily for experiments where no flow was necessary, as in cyclic voltammetry. A 5mm diameter hole was cut into a piece of PDMS and reversibly sealed to the electrode PDMS. The hole was filled with a drop of solution, covering the electrodes. The area of electrode exposed to solution here was ~1.25 mm^2. As noted in the next section, the chip was placed on top of the window of the detector, indicating that the electrodes possessed some degree of transparency since light was detected from the back of the electrode.

ECL Micro-Flow System. The microchip assembly was placed in a light-tight box above the window of a photon counting photomultiplier tube (PMT) (Electron Tubes Limited, photodetector module DM0043C) and attached to a potentiostat (CH Instruments, CHI model 600B series). Tubing was inserted into a hole in the flow channel (Tygon tubing, ID: 0.010 in.) and a pump (World Precision Instruments, Aladdin-1000) equipped with a syringe and tubing (FEP Teflon tubing, ID: 1/16 in.) was used to flow buffer into the flow channel over the electrode surface. A sample solution was injected into the flow of buffer using a loop injector (Rheodyne, model #7520, 500 nL rotor). Figure 1D-E shows a photograph and diagram of the microfluidic flow system. As sample solution flowed over the electrode and a potential was applied by the potentiostat, the light generated by the reaction at the working electrode was collected and quantified as “light counts”. The photon counts were digitized using a CT2 Counter/Timer (Electron Tubes). Light counts were collected in 0.1 s data channels. Before each experiment, PMT dark counts were collected to ensure that the system was light tight. Typical dark counts were at a rate of less than 50 counts per second.

The ECL data from an injection from the flow system onto the microchip was peak-shaped. The peak maximum was determined to be the analytical signal. Generally, three trials were collected for each data point, unless otherwise noted. The electrodes were equilibrated by running cyclic voltammograms in buffer then running 1-2 equilibration injections. This procedure lead to the highest precision in the data. For some cyclic voltammetry experiments, a syringe containing only a reagent solution in buffer was placed in the syringe pump. The nano-injector was bypassed and this solution was flowed directly over the electrodes. The flow was stopped during the data collection.

Reference electrode drift study. The microelectrodes were first equilibrated with the 0.15 M phosphate buffer solution (pH = 7.4) for two minutes. During these two minutes, four background cyclic voltammograms were obtained to ensure a stable background. After allowing the microelectrodes to equilibrate, the solution of 100µM tripropylamine in 4.0 mM $Ru(bpy)_3^{2+}$ was placed in the electrode well. A cyclic voltammogram was obtained for the solution. Following the completion of each CV scan, three minutes was allotted to allow for the diffusion layer in the solution well to replenish. After three minutes had passed, another CV was obtained of the same solution. This process was repeated until ten cyclic voltammograms had been obtained for the same solution. For each trial, the peak anodic and cathodic potential was recorded, as well as the peak anodic and cathodic current.

Acknowledgements

This publication was made possible by grants from the National Institute for General Medical Science (NIGMS) (5P20GM103427), a component of the National Institutes of Health (NIH), and its contents are the sole responsibility of the authors and do not necessarily represent the official views of NIGMS or NIH. The authors would also like to acknowledge funding from NASA (Nebraska Space Grant), the Creighton University Ferlic Summer Research Scholarship, and the Clare Boothe Luce Foundation. The authors would also like to thank Rachel M. Feeny, John B. Wydallis, and Meghan M. Mensack for providing the molds for fabricating microfluidic devices and electrodes. We would also like to thank the Creighton Chemistry Department and the College of Arts and Sciences.

Keywords: electrochemiluminescence; microfluidics; carbon electrodes; luminol; tris(2,2'-bipyridyl)ruthenium

[1] P.S. Dittrich, A. Manz *Nat. Rev. Drug Discov.* **2006,** *5*, 210-218.
[2] N. Nuchtavorn, W. Suntornsuk, S.M. Lunte, L. Suntornsuk *J. Pharmaceut. and Biomed.* **2015**, *113*, 72-96.
[3] J. Wang *Electroanalysis* **2005** *17*, 1133-1140.
[4] Y. Sameenoi, M.M. Mensack, K. Boonsong, R. Ewing, W. Dungchai, O. Chailapakul, D.M. Cropek, C.S. Henry *Analyst* **2011**, *136*, 3177-3184.
[5] X. Li, F. Zhang, J. Shi, L. Wang, J.-H. Tian, X.-T. Zhou, L.-M. Jiang, L. Liu, Z.-J. Zhao, P.-G. He, Y. Chen *Electrophoresis* **2011**, *32*, 3201-3206.
[6] Y. Liu, X. Huang, J. Ren *Electrophoresis* **2016**, *37*, 2–18.
[7] A.J. Bard, Electrogenerated Chemiluminescence, Marcel Dekker, New York, 2004.
[8] M.M. Richter *Chemical Reviews* **2004** *104*, 3003–3036.
[9] S.E.K. Kirschbaum, A.J. Baeumner *Anal. Bioanal. Chem.* **2015**, *407*, 3911–3926

[10] E.M. Gross, H.E. Durant, K.N. Hipp, R.Y. Lai *ChemElectroChem* **2017,** *4*, 1594–1603.
[11] P.W. Rhyne, O.T. Wong, Y.J. Zhang, R.S. Weiner *Bioanalysis* **2009**, *1*, 919-935.
[12] Y. Wang, D. Shan, G. Wu, H. Wang, F. Ru, X. Zhang, L. Li, Y. Qian, X. Lu *Biosens. Bioelectron.* **2018**, *106*, 64–70.
[13] N. Hao, X.L. Li, H.R. Zhang, J.-J. Xu, H.-Y. Chen *Chem. Commun*. **2014**, *50*, 14828–14830.
[14] R.L. McCreery *Chem. Rev.* 2008, 108, 7, 2646-2687.
[15] M. Brun, J.-F. Chateaux, A.-L. Deman, P. Pittet, R. Ferrigno *Electroanalysis* **2011**, *23*, 321-324.
[16] J. Gouyon, F. d'Orlyé, S. Griveau, F. Bedioui, A. Varenne *Electrochim. Acta.* **2020**, *329*, 135164.
[17] J. Li; M. Huang; X. Liu; H. Wei, Y. Xu, G. Xua; E. Wang *Analyst*, **2007**,*132*, 687-691.
[18] H. Al-Kutubi; S. Voci; L. Rassaei; N. Sojic; K. Mathwig *Chemical Science* **2018**, *9*, 8946-8950.
[19] K. Mathwig and N. Sojic *J. Anal. Test.* **2019**, *3*, 160-165.
[20] A. Onal *Food Chemistry* **2007**, *103*, 1475–1486.
[21] M.S. Burkhead; H. Wang; M. Fallet; E.M. Gross *Anal. Chim. Acta* **2008**, *613*, 152-162.
[22] G. Greenway; A. Knight; P. Knight *Analyst* **1995**, *120*, 2549-2552.
[23] C.A. Marquette, L.J. Blum *Anal. Bioanal. Chem.* **2008**, *390*, 155-168.
[24] W.R. Heineman and P.T. Kissinger in *Laboratory Techniques in Electroanalytical Chemistry*, *2nd ed*. (eds. P.T Kissinger and W.R. Heineman) Marcel Dekker, New York, **1996** pp 81-82.
[25] J.K. Leland and M.J. Powell *J. Electrochem. Soc.* **1990**, *137*, 3127-3131.
[26] Z. Chen and Y. Zu *J. Phys. Chem. C* **2008**, *112*, 42, 16663-16667.
[27] W. Miao, J.-P. Choi, A.J. Bard *J. Am. Chem. Soc.* **2002**, *124*, 48, 1447814485.
[28] M.-T. Chiang; M.-C. Lu; C.-W. Whang *Electrophoresis* **2003** *24*, 3033-3039.
[29] W. Guan; M. Liu; C. Zhang *Biosens. Bioelectron.* **2016**, *75*, 247-253.
[30] T. Hiroi; A. Inui; J. Jin; T. Takeuchi *Microchim Acta* **2006**, *154*, 269–274.
[31] R. Liu; C. Zhang; M. Liu *Sens. Actuators B: Chem.* **2015**, *216*, 255-262.
[32] M. Liu; R. Liu; D. Wang; C. Liu; C. Zhang *Lab Chip* **2016**, *16*, 2860–2870.
[33] T. Kuwana, B. Epstein, E. Seo *J. Phys. Chem.* **1963**, *67*, 2243-2244.
[34] C.A. Marquette, L.J. Blum *Anal. Bioanal. Chem.* **2006**, *385*, 546-554.
[35] H. Cui, G-Z Zou, X-Q Lin *Anal. Chem*. **2003**, *75*, 324-331.
[36] J.E. Vitt, D.C. Johnson, R.C. Engstrom *J. Electrochem. Soc.* **1991,** *138*, 1637-1643
[37] A. Wroblewska, O.V. Reshetnyak, E.P. Koval'chuk, R.I. Pasichnyuk, J. Blazejowski *J. Elctroanal. Chem*. **2005**, *580*, 41-49.
[38] C.A. Marquette, L.J. Blum *Anal. Chim. Acta* **1999**, *381*, 1-10.
[39] M. Alvarez-Icaza, U. Bilitewski *Anal. Chem*. **1993**, *65*, 525A-533A.
[40] M. Liu; D. Wang; C. Liu; R. Liu; H. Li; C. Zhang *Sens. Actuators B: Chem.* **2017**, *246*, 327–335.
[41] C.A. Marquette, B.D. Leca, L.J. Blum *Luminescence* **2001**, *16*, 159-165.
[42] B.D. Leca, A.M. Verdier, L.J. Blum *Sens. Act. B* **2001**, *74*, 190-193.
[43] A. Sassolas A, L.J. Blum, B.D. Leca-Bouvier *Anal. Bioanal. Chem.* **2009**, *394*, 971-980.
[44] Z. Zhou, L. Xu, S. Wu, B. Su *Analyst* **2014**, *139*, 4934-4939.
[45] G. Ma, J. Zhou, C. Tian, D. Jiang, D. Fang, H. Chen *Anal. Chem.* **2013**, *85*, 3912-3917.
[46] D.C. Duffy, J.C. McDonald, O.J.A. Schueller, G.M. Whitesides, *Anal. Chem.* **1998**, *70*, 4974–4984.

Entry for the Table of Contents

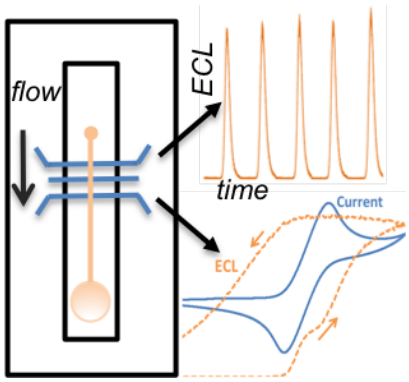

Electrochemiluminescence (ECL) was generated on novel microfluidic devices with carbon paste microelectrodes. ECL was generated using reactions involving tris(2,2'-bipyridyl)ruthenium(II) and luminol. These carbon paste microelectrodes are easily modifiable and have many possibilities for ECL-based detection methods on microfluidic devices.